

RESEARCH ARTICLE

Emissions from diesel versus biodiesel fuel used in a CRDI SUV engine: PM mass and chemical composition

Jitendra Gangwar¹, Tarun Gupta², Sudhir Gupta¹, and Avinash K. Agarwal¹

Departments of¹Mechanical and ²Civil Engineering, Indian Institute of Technology Kanpur, Kanpur, Uttar Pradesh, India

Abstract

The diesel tailpipe emissions typically undergo substantial physical and chemical transformations while traveling through the tailpipe, which tend to modify the original characteristics of the diesel exhaust. Most of the health-related attention for diesel exhaust has focused on the carcinogenic potential of inhaled exhaust components, particularly the highly respirable diesel particulate matter (DPM). In the current study, parametric investigations were made using a modern automotive common rail direct injection (CRDI) sports utility vehicle (SUV) diesel engine operated at different loads at constant engine speed (2400 rpm), employing diesel and 20% biodiesel blends (B20) produced from karanja oil. A partial flow dilution tunnel was employed to measure the mass of the primary particulates from diesel and biodiesel blend on a 47-mm quartz substrate. This was followed by chemical analysis of the particulates collected on the substrate for benzene-soluble organic fraction (BSOF) (marker of toxicity). BSOF results showed decrease in its level with increasing engine load for both diesel and biodiesel. In addition, real-time measurements for organic carbon/elemental carbon (OC/EC), and polycyclic aromatic hydrocarbons (PAHs) (marker of toxicity) were carried out on the diluted primary exhaust coming out of the partial flow dilution tunnel. PAH concentrations were found to be the maximum at 20% rated engine load for both the fuels. The collected particulates from diesel and biodiesel-blend exhaust were also analyzed for concentration of trace metals (marker of toxicity), which revealed some interesting results.

Keywords: Diesel Particulates, CRDI engine, Benzene soluble organic fraction, Elemental carbon, Organic carbon, Polycyclic aromatic hydrocarbon.

Introduction

Diesel engines are extremely versatile with a very high power-to-weight ratio. In addition to inherent high efficiency leading to low emission levels of carbon dioxide (CO₂), diesel engines produce low carbon monoxide (CO) and hydrocarbons (HC) exhaust levels. Despite all these advantages, diesel engines have disadvantages in terms of high NO_x and particulate matter (PM) emissions, which are directly associated with adverse human health and environmental impacts. Vehicular traffic makes a major contribution to both gaseous and particulate emission, and of toxic species such as benzene and polycyclic aromatic hydrocarbons (PAHs), and metals. The complexity of physical and chemical properties of diesel aerosols is constantly changing with the implementation of advanced diesel emission

control technologies (Johnson et al. 1992; Gupta et al. 2010). The size distribution and chemical composition of PM can vary greatly depending on the engine type, engine speed and load, fuel injection equipment type, compositions of fuel, lubricating oil and emission control technology (CAL EPA 1998, Hare (1997)). The properties of PM also changes with their residence time in atmosphere, because they undergo transformation once released in the atmosphere or while in the measurement apparatus such as dilution tunnel. Such transformations include particle coagulation, evaporation, and/or condensation of volatile organic compounds. Diesel particulate matter (DPM) has a very large surface area/volume ratio, which makes it an excellent carrier for adsorbed inorganic and organic species. Diesel exhaust particulates are a complex

Address for Correspondence: Dr. Avinash K. Agarwal, Department of Mechanical Engineering, Indian Institute of Technology Kanpur, Kanpur-208016, Uttar Pradesh, India. Tel: +91 512 2597982. Fax: +91 512, 2597408. E-mail: akag@iitk.ac.in

(Received 05 January 2011; revised 29 March 2011; accepted 14 April 2011)

mixture of hundreds of constituents present in both gaseous and aerosol phases. In the gaseous phase, the major constituents of diesel exhaust are nitrogen, oxygen, CO₂, CO, water vapor, nitrogen compounds, sulfur compounds, and low-molecular-weight hydrocarbons. Among these, the most toxic are formaldehyde, acetaldehyde, acrolein, benzene, 1,3-butadiene, PAHs, and nitro-PAHs. The solid phase emissions are primarily nuclei mode (10–80 nm) spherical carbon particles; these are termed as solids (SOL), solid particulate, or soot (Vuk et al. 1976; Frisch et al. 1979). Approximately 90% of the mass for diesel particulates exist as two distinct submicron modes: a nuclei mode (7.5–56 nm) and an accumulation mode (56–1000 nm) (Johnson et al. 1992). These nanoparticles have very large surface area per unit mass, and may easily become coated with contaminants that include toxic metals (lead, cadmium, arsenic, chromium, zinc), sulfur, and PAHs (Cass et al. 2000). About 90% of DPM are present in a size range from 7.5 to 1000 nm (Gupta et al. 2010); these particles are important in terms of potential health impact due to their ability to be inhaled and get deposited in the bronchial passages and alveoli of the lungs. The liquid phase emissions are composed of the organic or hydrocarbon compounds and sulfates. Some of hydrocarbons get absorbed/condensed onto the SOL, whereas some may still remain in the gas phase. Sulfates and trace metals are of prime concern among the inorganic constituents of DPM. Typically, a four-stroke heavy-duty engine emits metallic components such as silicon, calcium, zinc, and phosphorus (Springer 1997; Dwivedi et al. 2006; Agarwal et al. 2010). Calcium was found to be a dominant metal in PM with levels ranging from 0.01% to 0.29% (w/w_{particulate}). Phosphorus, silica, and zinc were next most metallic elements found and sodium, iron, nickel, barium, chromium, and copper were present either in small concentrations or were below detection limits (Agarwal et al. 2010). Valavanidis et al. (2000) indicated that the deposition of metals (especially Fe) on the lower airway would generate hydrogen radicals first and then trigger the production of oxygen free radicals and finally causes both acute and chronic lung injuries. Therefore, it is expected that besides the organic content and particulate matter, the investigation of metal contents in the engine exhaust is important for assessing potential health effects associated with diesel exhaust. Epidemiological studies carried out by various researchers have been reviewed and a strong link is established between occupational exposure to diesel particulates and lung cancer (HEI 1995, Wichmann and Peters (2000)). Animal studies generally support these finding and demonstrate that exposure to diesel particulates and other nanoparticulate forms of carbon are carcinogenic (Heinrich et al. 1995) but these finding are complicated by the issue of rat lung overload (Workshop ILSI 2000).

The organic fraction comes from the unburnt fuel and lubricating oils, and from partially oxidized/

pyrolyzed fuel and oils (Williams et al. 1987). Organic fraction containing neutral and aromatic fraction of diesel soot is mutagenic and carcinogenic in nature (USEPA 1995). A composite indicator of toxic potential of organic fraction compounds present in the PM is benzene-soluble organic fraction (BSOF). The organic fraction of diesel particulates contain compounds such as aldehydes, alkanes and alkenes, aliphatic hydrocarbons, PAH and PAH derivatives (Johnson et al. 1994; Cheung et al. 2010).

In contrast with diesel emissions, scientists are constantly working on alternative fuels, to help address energy cost, energy security, and global warming concerns associated with liquid fossil fuels. Biofuel's contribution to greenhouse effect is almost negligible, since CO₂ emitted during combustion is recycled in the photosynthesis process in the plants (Narayana 1992; Bona et al. 1999; Agarwal and Agarwal 2007). Amongst alternative fuels, biodiesel has shown great potential, especially to address the problem of CO₂ emissions (global warming) and need for decentralized power, especially in rural areas (Wedel 1999). Biodiesel has advantages of being virtually free from sulfur and aromatic compounds; therefore, the possibility of its particulates being less toxic is contemplated; however, it needs to be experimentally verified. A number of studies of larger heavy-duty engines and vehicles have concluded that biodiesel can provide emission reduction in terms of HC, CO, and PM, with some increase observed for nitrogen oxides (NO_x) (Turrio-Baldassarri et al. 2004). Biodiesel has higher cetane number than mineral diesel because of its higher oxygen content. It reduces the ignition delay thus combustion starts earlier and therefore emissions of HC, CO, and PM are reduced due to higher premixed combustion. Biodiesel can be used alone (B100) or can be blended with petroleum diesel in any proportions (Amann et al. 1980; CARB 1998; Agarwal et al. 2006). Biodiesel (20%) blended with mineral diesel (80%) is one of the most popular biodiesel blends investigated and recommended world over. Biodiesel for the present experimental study was produced from karanja oil (*Pongamia pinnata*) using transesterification process.

The objective of this paper is to comparative assess and characterize of particulate emissions from a common rail direct injection (CRDI) engine fuelled with mineral diesel and B20 (20% biodiesel blend) exhaust in terms of (i) BSOF, (ii) PAHs, and (iii) trace elemental metals.

Experimental setup

For the comparative study of biodiesel and mineral diesel, a CRDI sports utility vehicle (SUV) diesel engine (Make: Tata, Pune, India; Model: Safari Dicor 3.0 L) was employed. The engine was ~1 year old and had done ~15,000 km at the beginning of this set of experiments. The engine used a high pressure fuel pump and a common rail system for supply of fuel to all the cylinders at

very high injection pressures up to 1600 bars. The injectors were controlled electronically using electronic control unit (ECU). The fuel injection pressure was controlled by the pre-programmed ECU. The fuel injection pressures were modulated by ECU with changing engine load and speed. High fuel injection pressures resulted in better atomization of the fuel sprays, which led to more complete combustion, higher efficiency, and lower emissions. The engine was coupled with an eddy current dynamometer for loading the engine at different speeds (Figure 1). The dynamometer was controlled using a dynamometer controller as well as a computer with software interface. The specifications of the engine and dynamometer used in the experimental setup are given in Table 1.

An experimental setup was developed, which included a set of different measuring instruments like semicontinuous organic carbon/elemental carbon (OC/EC) analyzer (Make: Sunset Laboratory, USA; Model: Semicontinuous field v.4), which measures organic carbon, elemental carbon, and total carbon (Bae et al. 2004); Online PAH analyzer (Make: EcoChem Labs, USA; Model: PAS 2000) (Ott and Siegmann 2006), which measures total particulate bound PAHs for primary as well as secondary aerosols, and emission analyzer (Make: AVL, India; Model: Digas 4000). A partial flow dilution tunnel was used for dilution of diesel exhaust emissions with ambient air in order to complete the coagulation and condensation processes occurring during the particulate formation. When the diesel engine was operated, carbonaceous soot particles and high boiling point hydrocarbons were emitted from the tailpipe. These hydrocarbons condense on soot (mostly EC) to form PM after being diluted with preheated air inside the partial flow dilution tunnel (Dwivedi et al. 2006). The schematic of the experimental setup developed for carrying out the engine experiments is given in Figure 2.

Engine exhaust flows through partial flow dilution tunnel before entering different instrument inlet as shown in Figure 2. Experimental setup was developed using pipes, elbows, and valves (Swagelok fittings) made

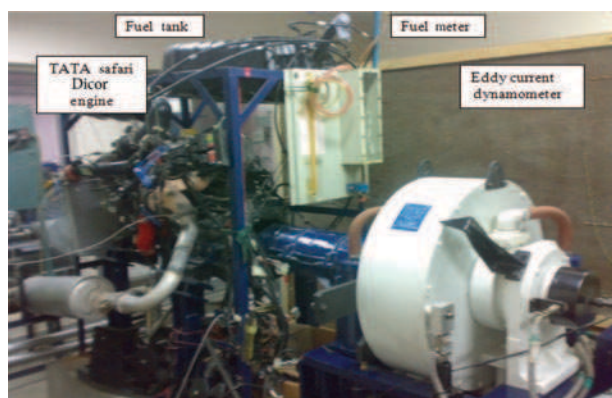


Figure 1. Tata Dicor common rail direct injection (CRDI) engine coupled with eddy current dynamometer.

of stainless steel (SS, grade 316), in order to ensure minimum contamination during experiment due to the inert nature of SS. Valves were installed at different places to control and distribute required exhaust aerosol flows to the instruments at different times of experiment. From the main exhaust pipe of the engine, small fraction of exhaust gas was passed on to a partial dilution tunnel. The whole setup was tested for leaks. Flows in different sections were measured using a mass flow meter. Thereafter, preheated and pre-filtered atmospheric air was mixed with this partial exhaust to attain a specific dilution ratio as specified by EPA (maintained between 10 and 16 in this case). The sample gas was mixed with ambient air inside the dilution tunnel, maintained at higher temperatures. As the mixture moves in the dilution tunnel, mixing and agglomeration processes of particulate formation are completed to a reasonable extent without abrupt condensation of vapor. This diluted gas then passes through the filter assembly, where particulates are filtered out on a preconditioned filter paper. A four-way valve was installed through which, undiluted exhaust was passed from one side, and on the other side diluted exhaust comes out. From the third side ambient air was passed. Finally, the exit line of four-way valve was connected to exhaust gas emission analyzer (Make: AVL, Austria; Model: 4000 Digas). This analyzer measures CO₂, CO, HC, NO_x, and O₂ in the engine exhaust. The CO₂ concentration was measured for undiluted exhaust, ambient air, and diluted exhaust for the calculation and verification of dilution ratio using the formulae given below:

$$\frac{[\text{Undiluted exhaust CO}_2]}{[\text{Diluted exhaust CO}_2 - \text{Ambient air CO}_2]}$$

Table 1. Engine and eddy current dynamometer specifications.

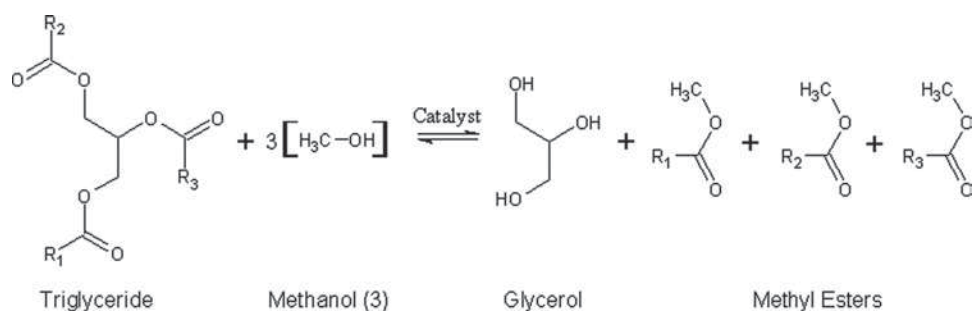
Engine specifications	
Make/Model	Tata, Pune, India/Safari Dicor 3.0 L (BS-III/Euro-III)
Engine type	Water cooled, CRDI, Turbocharged, Intercooled
No. of cylinders	4, In-line
Bore/stroke	97/100 mm
Cubic capacity	2956 cc
Maximum engine output	84.5 kW @ 3000 rpm
Maximum torque	300 Nm at 1600–2000 rpm
Compression ratio	17.5
Firing order	1-3-4-2
Fuel injection system	CRDI with 1600 bar max fuel injection pressure
Timing and governing	
	ECU control
Dynamometer specifications	
Make/Model	Dynamerik, Pune, India/EC-300
Capacity	220 kW at 2500–8000 rpm
Maximum speed	8000 rpm
Maximum torque	702 Nm
Direction of rotation	Bidirectional
RPM accuracy	±1 rpm

One line from partial flow dilution tunnel was passed through the real-time online instruments (PAS 2000, OC/EC Analyzer) for measuring the PAHs and elemental carbon, organic carbon, and total carbon in the exhaust. The volume of exhaust flow passing through these instruments was controlled by separate two-way valves.

Materials and methods

Fuel preparation and characterization

Biodiesel for the present experimental study was produced from karanja oil (*Pongamia. pinnata*) using transesterification process. The chemical reaction of transesterification process is shown below.



During the transesterification process, the triglyceride (vegetable oil) is reacted with alcohol in the presence of a strong catalyst, usually a strong alkali like KOH. High-grade methanol (6:1 molar ratio) is mixed with the alkali catalyst NaOH (1% w/w_{oil}) and added to the reactor containing heated vegetable oil. The transesterification reaction is normally carried out at 55–60°C at a stirring speed of 700–800 rpm for 1 h (Agarwal (1998)). After completion of the reaction, the reaction products are transferred to the separating flask, where upper phase, that is, biodiesel is separated from glycerol followed by subsequent washing (by distilled water) and drying process.

Four important tests were conducted according to ASTM standards on mineral diesel, biodiesel (B100), and biodiesel blend with diesel (B20) to analyze their kinematic viscosity, flash point temperature, density, and calorific value. Viscosity was measured by ASTM D 445 procedure. Setavis kinematic viscometer was used for the purpose, which is a glass capillary viscometer. The viscosity of biodiesel was found to be within the ASTM limits 1.9–6.0 cSt at 40°C. The flash point of a volatile liquid is the lowest temperature at which it can vaporize to form an ignitable mixture in air. The flash point is measured according to ASTM D 93. Flash point was measured by flash point tester (Model: 33000-0; Make: Sanhope-Seta, UK). 0.2 mL sample of each fuel was injected into the instrument after setting the temperature and then it was left for 120 sec. If the flash could be achieved by exposing a ignition source to the fuel vapors, the temperature was noted as flash point temperature. Otherwise, the experiment was repeated

for higher point temperature with a fresh sample. A bomb calorimeter (Model: 6200; Make: Parr, UK) was used to measure the heat of combustion of biodiesel and diesel samples. After calibration with benzoic acid, 0.5 to 1 g sample of each fuel was ignited in the combustion bomb. The reaction takes place at constant volume in a stainless steel combustion bomb. The sample was ignited in pressurised oxygen atmosphere. The bucket and bomb together constitute the reaction chamber. The bomb calorimeter measures the enthalpy of combustion under constant volume conditions. This exothermic reactions increase the temperature inside the bomb, which then transfers the energy to the external water jacket raising its temperature. It is this rise in the

water jacket temperature, which is monitored to obtain the energy release by the combustion reactions in bomb calorimeter. Specific gravity was measured by using high precision digital density meter (Model: DA-130N; Make: Kyoto Electronics, Japan). A small volume of liquid sample was introduced into an oscillating sample tube and the change in the oscillating frequency caused by the change in the mass of the tube was used in conjunction with calibration data to determine the density of the sample (ASTM D 4052) at prescribed conditions.

Engine experiments and particulate sampling

To characterize the emissions from mineral diesel and biodiesel (B20), the engine was operated at loads ranging from 0%, 20%, 40%, 60%, 80%, and 100% of rated engine load at constant speed of 2400 rpm. This engine speed typically represents high-speed highway driving conditions. Particulate samples were collected isokinetically using a partial flow dilution tunnel. The partial flow dilution tunnel was used to simulate the ambient environment for collecting the exhaust particulates from engine (Dwivedi et al. 2006). This tunnel draws a fraction of exhaust gases out from the main exhaust line. Thereafter, pre-filtered and preheated atmospheric air was mixed with this partial exhaust gas to attain a dilution ratio between 10:1 and 16:1. The sample gas was then mixed with filtered and conditioned ambient air inside the dilution tunnel. The diluted exhaust undergoes complete mixing and particulate formation steps via condensation of gaseous material on tiny nuclei particles (heterogeneous condensation) along with adsorption, absorption, agglomeration, and coagulation processes, which are completed to a reasonable extent

within the designed residence time inside the dilution tunnel. When the diesel engine is operated, carbonaceous soot particles and high boiling point hydrocarbons are emitted from the tailpipe. These hydrocarbons condense on soot to form PM after being diluted with preheated air inside the partial flow dilution tunnel. This mature soot is then collected using the following sampling details for various investigations and analyses.

The first step in the sampling procedure was conditioning and preparation of filter papers (Make: Whatman; 47 mm, Tissue-Quartz Filter). Filter papers were first desiccated for 12 h in anhydrate silica gel desiccators and then weighed using a microbalance (Make: Mettler, Toledo). For collecting the particulate sample, pre-weighed, conditioned filter paper was placed in filter holder assembly of the partial flow dilution tunnel. The engine was operated for a predetermined period of time at desired load and speed, and particulates were collected on the filter substrate (Table 2). After completion of the engine experiment, the filter substrate was carefully removed from the filter assembly and kept in the desiccator for 12 h and then weighed again. These filter papers were then further analyzed for total mass of particulates collected, BSOF, and trace elemental metals as per the test plan. The samples

were collected only once on the filter papers but they were analyzed three times. The experimental error was within a standard deviation of 2%; therefore, average values are reported in the article.

Real-time measurements

All the instruments were calibrated and tested individually with ambient air before carrying out the engine experiments. The semicontinuous OC/EC analyzer measures organic carbon, elemental carbon, and total carbon. OC/EC instrument provides organic and elemental carbon results, which are comparable with the recognized NIOSH method 5040. Once the sample collection is completed, the oven is purged with helium. This is followed by a stepped-temperature ramp, which increases the oven temperature to 850°C, thus thermally desorbing OC and pyrolysis products enter into a manganese dioxide (MnO₂) oxidizing oven. As the carbon fragments flow through the MnO₂ oven, they are quantitatively converted to CO₂. The CO₂ is swept out of the oxidizing oven along with helium stream and measured directly by a self-contained non-dispersive infrared (NDIR) detector system. A second temperature ramp is then initiated in an oxidizing gas stream and

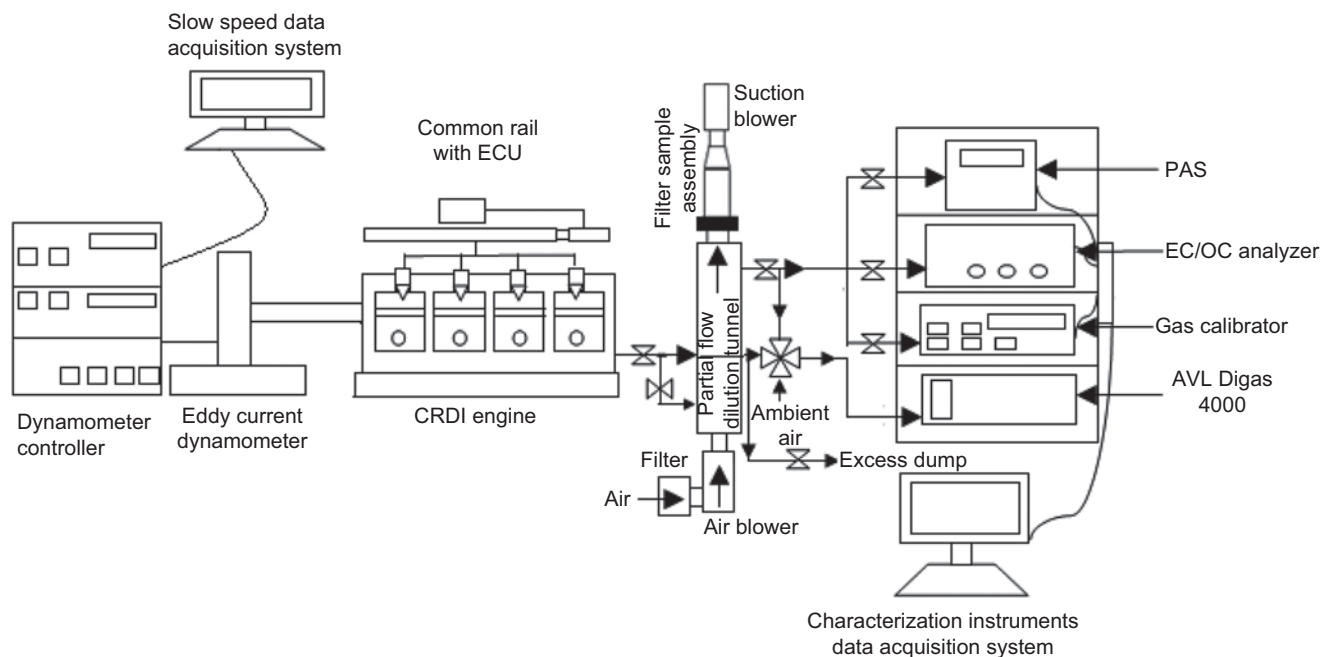


Figure 2. Schematic of the experimental setup.

Table 2. Sampling details.

Engine speed (rpm)	Engine load (%)	Sampling duration for mass/BSOF (min)	Online sampling duration for OC/EC (min)	Online sampling duration for PAHs (min)	Sampling duration for metals (min)
2400	0	30	5	5	15
2400	20	30	5	5	15
2400	40	30	5	5	15
2400	60	30	5	5	15
2400	80	30	5	5	15
2400	100	30	5	5	15

then elemental carbon is oxidized off the filter and into the oxidizing oven and NDIR. The EC is then detected in the same manner as the OC (Bae et al. 2004).

The Photoelectric Aerosol Sensor (PAS) is a standard real-time monitor for particle-bound PAHs measurement, which works on the principle of photoionization of particle-bound PAHs. PAH analyzer measures total particulate bound PAHs for primary exhaust particulates in the present study. The PAS responds to photoemitting substances on the surface of aerosol particles. Ultraviolet irradiation of the sampled aerosol led to the emission of photoelectrons from the surface that readily undergoes photoemission. The remaining positively charged aerosol particles were separated from the electrons and collected on a filter connected to an electrometer. The measured current was a function of the UV irradiation wavelength and intensity, the total available surface area, and the photoemission properties of the surface.

BSOF analysis procedure

ASTM test method D4600-87 (ASTM 2001) was used for estimation of BSOF in diesel particulates. This gravimetric method was recommended by National Institute of Occupational Safety and Health (NIOSH), USA to represent the toxic organic compounds present in the particulates collected on filter paper. Filter papers were desiccated for 12 h before and after sampling and initial and final weights were noted. Filter papers were cut into several small pieces using a metal scissor and then placed into a reagent beaker. Thereafter, 20 mL of benzene was added to it. These reagent bottles were kept in ultrasonic bath for 20 min. Thereafter, sample was decanted and vacuum-filtered through 0.45 µm Millipore filter paper. The filtrate was collected in a 100-mL pre-weighed beaker. The procedure was repeated with another 10 mL of benzene in the same reagent beaker. These 100-mL beakers were covered with aluminum foil having holes and were kept in oven at 40°C for 12 to 18 h until the sample dried. The initial and final weight of the beaker was measured at room temperatures to estimate the total mass of BSOF in the sample. In order to check the reference concentration, blank filters were used for benzene extraction as per the same ASTM standard.

Trace metal analysis procedure

The particulate samples collected on the filter substrate need to be analyzed for detection of elemental trace metals using the inductively coupled plasma optical emission spectrometry (ICP-OES) (Make: Thermo Fischer Scientific; Model: iCAP DUO 6300 ICP Spectrophotometer). It is a type of emission spectroscopy that uses inductively coupled plasma to produce excited atom and ions that emit electromagnetic radiations at characteristic wavelength of a particular element. The intensity of this emission is indicative of the concentration of the element present in the sample. The details of elemental analysis via ICP-OES can be found elsewhere (Chakraborty and Gupta 2010).

USEPA, SW-846, 3015 method was used for extracting trace metals from DPM. Sample extraction was carried out using hot plate digestion method. This digestion procedure is used for preparing samples, which are to be analyzed by ICP-OES. One half of the sample laden filter was cut into small pieces using plastic scissor and then put into an inert bottle, in which 15 mL concentrated HNO₃ was added. The remaining half of the filter paper was taken in similar way into another bottle. Temperature of each sample was raised to 175°C in <5.5 min and maintained at 175°C for >4.5 min. After digestion, the acid from the two vessels was taken together and filtered through 0.22 µm filter paper. The filtrate was measured and diluted three times with Milli-Q water and then further stored in inert bottles. Analytical blank filter paper and 30 mL of concentrated HNO₃ (Suprapure, Merck) were taken as references (Chakraborty and Gupta 2010). The 10% of blanks from the same lot of filter papers were used to get a representative average blank concentration for data correction. By this method, concentrations of trace metals such as Ca, Cu, Cr, Fe, Na, Ni, Pb, Zn, Mn, Mg were analyzed using ICP-OES.

Results and discussions

The measured physical properties of biodiesel and mineral diesel are shown in Table 3.

Figure 3 shows the particulate mass collected on the filter paper from diesel and biodiesel (B20) exhaust from CRDI engine at varying load conditions (on the primary axis). Particulate mass was collected on the filter substrate after sampling for 30 min (Table 2). Figure 3 shows that the particulate mass increases with increase in engine load for both fuels, biodiesel and mineral diesel. As the load increases, more fuel undergoes combustion resulting in higher formation of the primary diesel exhaust particulate formations. In Figure 3, it can also be noticed that the mass emission of particulates collected in the partial flow dilution tunnel is lower for biodiesel blend. This is because of higher oxygen content in biodiesel, which is blended with mineral diesel, leading to relatively lower particulate formation after the combustion and improvement in emission characteristics.

The particulate-loaded filter papers (containing diesel and biodiesel exhaust particulates collected at different engine load conditions) were then analyzed for BSOF content. The results are shown in Figure 3 on the secondary axis. It can be noted that at no load condition, the BSOF of the particulate is highest among all compared with other engine loads, both for

Table 3. Measured physical properties of diesel and biodiesel.

Fuel property	Diesel	B20	B100
Specific gravity	0.846	0.848	0.899
Kinematic viscosity (cSt) at 30°C	2.60	3.39	5.81
Calorific value (MJ/kg)	42.21	38.28	36.32
Flash point (°C)	52	79	190

diesel as well as biodiesel. This is possibly due to relatively lower in-cylinder combustion temperature and incomplete combustion occur at no load condition, which favors higher OC formation primarily because of partially burnt fuel and lubricating oil contributions to the particulates. As the engine load increases, the air-fuel ratio moves closer to stoichiometric leading to more complete combustion because of higher in-cylinder temperature and consequently results in lower amount OC formation in the combustion chamber. This can be clearly noted from Figure 3 that the BSOF decreases steadily with increasing engine load. Soluble organic fraction of the particulate matter mainly consist of organic portion of fuel itself and pyrolytically generated organic products formed during the process of soot formation. As the load increases, SOF of particulate matter decreases. At higher engine loads, combustion efficiency is relatively better hence contribution from unburned fuel decreases thus BSOF of the PM also decreases. The main point to be noticed here is that for B20 particulates, the value of BSOF is higher than that of diesel particulates. This is primarily

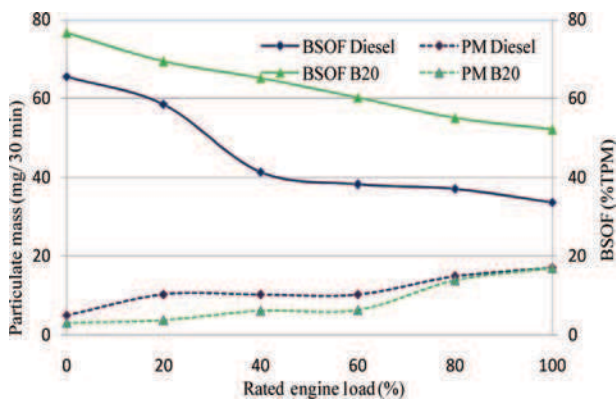


Figure 3. Particulate matter (PM) mass and benzene-soluble organic fraction (BSOF) of primary diesel and biodiesel exhaust particulates from common rail direct injection (CRDI) engine at 2400 rpm.

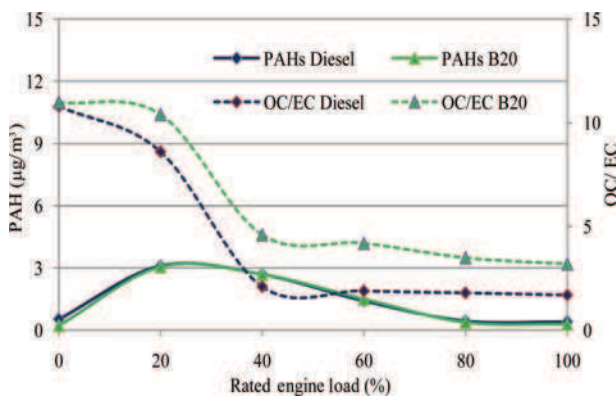
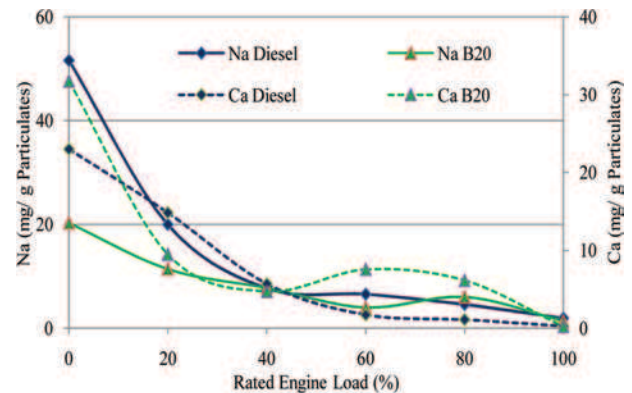


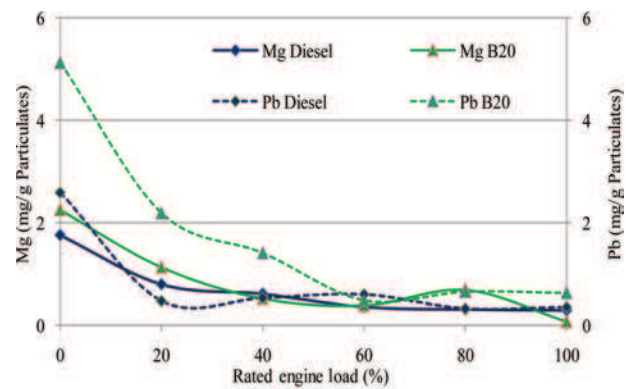
Figure 4. Polycyclic aromatic hydrocarbons (PAHs) and organic carbon/elemental carbon (OC/EC) ratio in primary diesel and biodiesel exhaust particulates from common rail direct injection (CRDI) engine at 2400 rpm.

because of lower volatility of the constituents of biodiesel. The increased mass consist mostly of unburned esters from the fuel itself (Sharp et al. 2000). This needs to be further investigated experimentally and verified by animal exposure studies, before going for large-scale implementation of biodiesel program around the world.

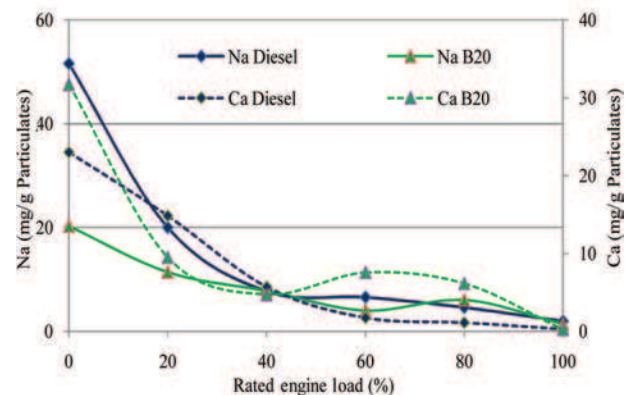
Figure 4 shows the time-averaged PAH concentrations present in the diesel exhaust particulates from CRDI engine at varying load conditions. This figure



(a)



(b)



(c)

Figure 5. Trace metal content in primary engine exhaust particulate from diesel and biodiesel-fueled common rail direct injection (CRDI) engine at 2400 rpm.

shows the time-averaged ratio of OC/EC for primary diesel and biodiesel exhaust particulates for different engine loads.

PAHs originate either from the fuel itself or result from the pyrolysis of fuel/lubricating oil/OC formed within the combustion chamber. As it can be seen from Figure 4, the PAHs concentration is low at no load conditions possibly due to lower combustion temperatures that prevent extensive pyrolysis and cyclization resulting in lower PAH formation. The peak concentrations for PAHs are visible at 20% load indicating that at this load, high enough combustion temperatures are attained, which favor formation of highest amount of PAHs. As the engine load increases further, the combustion takes place at even higher temperature resulting in relatively lesser amounts of OC being produced. Since OC are important precursors for PAHs, this causes further reduction in overall production of the PAHs in the engine exhaust. At higher engine loads, the in-cylinder combustion temperature is relatively higher. At higher temperature, there is a strong possibility of reburning of the PAHs formed; therefore, lower PAHs emission from the engine tail pipe is observed at higher engine loads. Another possible reason for relatively lower PAHs at higher engine loads could be the migration of particle-bound PAHs to the gas phase, and lesser PAH condensation due to increasing overall combustion temperatures and exhaust gas temperatures.

Figure 5 shows the trace metal content of the particulate collected on the filter paper from diesel and biodiesel (B20) exhaust from CRDI engine at varying load conditions. Various metals were investigated; however, many of the metals were below the detection limit of the instrument and only the metal detected with reasonable confidence in the data are reported here. The data was subjected to blank correction and the metals are represented in the form of mg/g of particulate collected on the filter paper. The main metals detected were Na, Ca, Cu, Mn, Mg, and Pb, which are given in Figure 5.

Table 4 shows measured concentrations of Na, Ca, Cu, Mn, Mg, and Pb in diesel, biodiesel blends (B20), and lubricating oil. The metal content in the fuel samples and lubricating oil are distinct from each other, for example, calcium was found to be lower in B20 compared with mineral diesel, whereas manganese was found to be higher. There are factors like lubricity of the fuel, which affects the wear of fuel injection system and other vital engine components thus changing the presence of wear metals in particulate.

Table 4. Concentration of various metals in diesel, biodiesel, and lubricating oil samples.

Metals	Diesel ($\mu\text{g/g}$)	B20 ($\mu\text{g/g}$)	Lubricating oil ($\mu\text{g/g}$)
Na	39.3	21.62	66.98
Ca	33.1	28	59.4
Pb	9	17	12
Mg	5.8	7.4	18.9
Cu	9	7.3	3.4
Mn	1.2	2	1

It is visible from Figure 5A that Na concentration is very high compared with any other metal. At 2400rpm, the concentration of Na and Ca from diesel was observed to be higher than B20 exhaust, which is possibly due to the presence of higher amount of sodium and calcium in diesel compared to biodiesel as depicted from Table 4. Figure 5B shows concentration of Pb and Mg in particulate from diesel and B20 exhaust. At 2400rpm, both metals show higher concentration for B20 exhaust. This is due to their higher concentration in the fuel (Table 4). Figure 5C shows Cu and Mn concentration in particulates from diesel and B20 exhaust at 2400rpm. It is visible from graph at 2400rpm B20 exhaust shows higher concentration of Mn compared to diesel at all loads but Cu concentration was higher for mineral diesel exhaust at 0% load and as load increases, Cu concentration from B20 exhaust increases. This can also be explained with the help of Table 4. These results hold significant importance as earlier results from toxicological studies have revealed that copper, zinc, and vanadium emitted from various combustion processes were linked to increase in blood fibrinogen resulting in cardiovascular health effects (Ghio et al. 2000; Ghio and Huang 2004).

Overall, it can be seen from Figure 5 that all the metals present in the particulates of B20 and diesel follow the same trend as their fuel. They have highest concentration of metals at lower engine loads with a continuously decreasing trend with increase in engine load. It is also reported by Sharma et al. (2005) that overall particulate formation increases in the form of elemental carbon with increase in engine load. At higher engine loads, higher amount of fuel is being injected and burnt in the engine that results in high particulate matter emission. For this reason, the particulate emission from the diesel engine is higher but the corresponding metal content is lower for higher engine loads. The previous study by Ullman (2004) showed that at higher engine loads, particulate emission is more in terms of elemental carbon, thereby reducing metal content (mg/g) in the particulates. It is also visible from graph that the trace metal content of particulates from biodiesel (B20)-fueled engine is relatively higher compared with mineral diesel fuelled engine. This indicates possibly relatively higher metal toxic potential for the particulates from biodiesel-fueled engine compared with mineral diesel-fueled engine.

Summary

Parametric investigations were carried out using an automotive CRDI diesel engine operated at different loads at constant engine speed (2400rpm), employing diesel and 20% biodiesel blends (B20) produced from karanja oil for PM mass, BSOF, EC/OC, total PM-bound PAHs, and trace metals. Biodiesel blend (B20) showed superior engine performance in reducing particulate mass emission at all operating condition compared with mineral diesel. This may be due to lower sulfur and aromatic content of biodiesel. For B20, the BSOF content of particulates was found to be higher than that of mineral diesel. This may be primarily

because of relatively lower volatility of constituents of biodiesel, indicating possibly higher toxicity of biodiesel emissions. This agrees with earlier studies that have shown higher levels of formaldehyde (major BSOF component) levels in emissions from engine running on biodiesel blend (Bünger et al. 2000; Turrio-Baldassarri et al. 2004). The OC/EC graph showed that with increase in engine load, the ratio of OC to EC decreases. This is likely to happen because at higher temperatures, the amount of OC (organic species produced as a result of fuel pyrolysis) produced is lower or it gets another chance to get completely oxidized to CO₂ and water. This also suggests that with increasing engine load, the toxic potential of particulates actually decreases. It is observed from the results presented in this study that the PAHs concentration is low at no load conditions and it attains a maximum concentration at 20% rated load and then comes down with further increase in engine load. The possible reason for this can be lower in-cylinder combustion temperatures at no load, which prevent extensive pyrolysis and cyclization resulting in lower PAH formation. At 20% load, high enough combustion temperatures are attained, which favors formation of highest amount of PAHs. As the engine load increases further, the combustion takes place at even higher temperatures resulting in relatively lesser amounts of OC being produced. Since OC are important precursors for PAHs, this causes further reduction in overall production of PAHs in the engine exhaust. At higher in-cylinder combustion temperature, there is a strong possibility of reburning of the PAHs formed; therefore, lower PAHs emission from the engine tail pipe is observed at higher engine loads. Another possibility for relatively lower PAHs at higher engine loads could be the migration of particle-bound PAHs to the gas phase, and lesser PAH condensation due to increasing overall combustion temperatures and exhaust gas temperatures. These results are in agreement with earlier studies that showed most PAH emissions decreased as the average load and speed of the driving cycle increased (Karavalakis et al. 2010). They also found lower nitro-PAHs and higher oxy-PAH emissions with biodiesel blends. The PM collected from diesel and biodiesel exhaust were analyzed for elemental composition focusing on trace metals. The metal content in the particulates was found to be proportional to their concentration in the fuel itself. The concentrations of the metals analyzed showed a decreasing trend with increasing engine load. This indicates possibly higher metal toxicity potential for the particulates from biodiesel-fueled engine compared to mineral diesel-fueled engine. The results can be generalized for this generation of DI/CRDI engine with high fuel injection pressures.

In summary, in spite of having lower mass emission of particulates, the BSOF and trace metal content of particulates from biodiesel engine are relatively higher than that of mineral diesel, indicating possibly higher toxicity potential of biodiesel particulates. These need to be further investigated and verified by animal exposure studies, before going for large-scale implementation of biodiesel program around the world.

Acknowledgements

The authors would like to thank Technology Systems Group's program on "Alternate Fuels," Department of Science and Technology, Government of India for providing the research grant for carrying out this study.

Declaration of interest

The authors report no conflict of interest. The authors alone are responsible for the content and writing of the article.

References

- Agarwal AK. 1998. Vegetable oils versus diesel fuel: development and use of bio-diesel in a compression ignition engine. *TERI Inform Digest Energy (TIDE)* 8:191-203.
- Agarwal AK, Gupta T, Kothari A. 2010. Toxic potential evaluation of particulate matter emitted from a constant speed compression ignition engine: a comparison between straight vegetable oil and mineral diesel. *Aerosol Sci Technol* 44:724-733.
- Agarwal D, Agarwal AK. 2007. Performance and emissions characteristics of Jatropha oil (preheated and blends) in a direct injection compression ignition engine. *Appl Thermal Eng* 27:2314-2323.
- Agarwal D, Sinha S, Agarwal AK. 2006. Experimental investigation of control of NO_x emissions in biodiesel-fueled compression ignition engine. *Renewable Energy* 31:2356-2369.
- Amann CA, Stivender DL, Plee SL, Macdonald JS. 1980. Some rudiments of diesel particulate emissions. SAE 800251.
- ASTM. 2001. D-4600-87: Standard test method for determination of benzene soluble particulate matter in workplace atmosphere.
- Bae MS, Schauer JJ, DeMinter JT, Turner JR, Smith D, Cary RA. 2004. Validation of a semi-continuous instrument for elemental carbon and organic carbon using a thermal-optical. *Atmos Environ* 38:2885-2893.
- Bona S, Mosca G, Vamerli T. 1999. Oil crops for biodiesel production in Italy. *Renewable Energy* 16:1053-1056.
- Bünger J, Krahl J, Baum K, Schröder O, Müller M, Westphal G, Ruhnau P, Schulz TG, Hallier E. 2000. Cytotoxic and mutagenic effects, particle size and concentration analysis of diesel engine emissions using biodiesel and petrol diesel as fuel. *Arch Toxicol* 74:490-498.
- CAL EPA (California Environmental Protection Agency). 1998. Part B: Health Risk Assessment for Diesel Exhaust, Proposed Identification of Diesel Exhaust as a Toxic Air Contaminant. Office of Environmental Health Hazard Assessment (OHEEA).
- Cass GR, Hughes LA, Bhawe P, Kleeman MJ, Allen JO, Salmon LG. 2000. The chemical composition of atmospheric ultrafine particles. *Philos Trans R Soc Lond A Math Phys Sci* 358:2581-2592.
- CARB. 1998. Proposed Identification of Diesel Exhaust as a Toxic Air Contaminant, Part A: Exposure Assessment. Californian Air Resources Board, 103.
- Chakraborty A, Gupta T. 2010. Chemical characterization and source apportionment of submicron (PM₁) aerosol in Kanpur region. *Aerosol Air Qual Res* 10:433-445.
- Cheung KL, Ntziachristos L, Tzankiozis T, Schauer JJ, Samaras Z, Moore KF, Sioutas C. 2010. Emissions of particulate trace elements, metals and organic species from gasoline, diesel, and biodiesel passenger vehicles and their relation to oxidative potential. *Aerosol Sci Technol* 44:500-513.
- Dwivedi D, Agarwal AK, Sharma M. 2006. Particulate emission characterization of a biodiesel vs diesel-fuelled compression ignition transport engine: a comparative study. *Atmos Environ* 40:5586-5595.

- Frisch LE, Jonson JH, Leddy DG. 1979. Effects of fuels and dilution ratio on diesel particulate emissions. SAE 790417.
- Ghio AJ, Huang YC. 2004. Exposure to concentrated ambient particles (CAPs): a review. *Inhal Toxicol* 16:53-59.
- Ghio AJ, Kim C, Devlin RB. 2000. Concentrated ambient air particles induce mild pulmonary inflammation in healthy human volunteers. *Am J Respir Crit Care Med* 162:981-988.
- Gupta T, Kothari A, Srivastava DK, Agarwal AK. 2010. Measurement of number and size distribution of particles emitted from a mid-sized transportation multipoint port fuel injection gasoline engine. *Fuel* 89:2230-2233.
- Hare CT. 1997. Characterization of diesel engine gaseous particulate matter. Final report prepared by South West Research Institute Contract No. 68-02-1977.
- HEI. 1995. Diesel exhaust: a critical analysis of emission, exposure and health effects. A special report of the Institute's diesel working group, HEI research report.
- Heinrich U, Fuhst R, Rittinghausen S, Creutzenberg O, Bellmann B, Koch W, Levsen K. 1995. Chronic inhalation exposure of Wistar rats and 2 different strains of mice to diesel-engine exhaust. Carbon-black, and titanium-dioxide. *Inhal Toxicol* 7:533-556.
- Johnson HJ, Bagley ST, Gratz LD, Leddy DG. 1992. A review of diesel particulate control technology and emissions effects. SAE 940233.
- Karavalakis G, Fontaras G, Ampatzoglou D, Kousoulidou M, Stournas S, Samaras Z, Bakeas E. 2010. Effects of low concentration biodiesel blends application on modern passenger cars. Part 3: impact on PAH, nitro-PAH, and oxy-PAH emissions. *Environ Pollut* 158:1584-1594.
- Narayana R. 1992. Biomass (renewable) resources for production of material. *Chem Fuels* 476:1-10.
- Ott WR, Siegmund HC. 2006. Using multiple continuous fine particle monitors to characterize tobacco, cooking, wood burning and vehicular sources in indoor. *Atmos Environ* 40:821-843.
- Sharma, M., Agarwal, A.K., Bharathi, K.V.L., 2005. Characterization of exhaust particulate from diesel engine. *Atmospheric Environment* 39, 3023-3028.
- Sharp CA, Howell SA, Jobe J. 2000. The effect of biodiesel fuels on transient emissions from modern diesel engines, Part II—unregulated emissions and chemical characterization. SAE Paper No. 2000-01-1968.
- Springer KJ. 1997. Characterization of sulfate, odor, smoke, POM and particulates from light duty and heavy-duty diesel engines. Part IX, Prepared by South West Research Institute, EPA/460/3-79/007.
- Turrio-Baldassarri L, Battistelli CL, Conti L, Crebelli R, De Berardis B, Iamici AL, Gambino M, Iannaccone S. 2004. Emission comparison of urban bus engine fueled with diesel oil and 'biodiesel' blend. *Sci Total Environ* 327:147-162.
- Ullman TL. 2004. Diesel Emission Testing. Asian Vehicle Emission Control Conference, Beijing, China.
- USEPA. 1995. Health Assessment Document for Diesel Engine Exhaust, Environmental Protection Agency. Office of Research and Development, Washington DC, EPA/600/8-90/057, USA.
- Valavanidis A, Salika A, Theodoropoulou A. 2000. Generation of hydroxyl radicals by urban suspended particulate air matter. The role of iron ions. *Atmos Environ* 2379-2386.
- Vuk CT, Jones MA, Johnson JH. 1976. The measurement and analysis of the physical character of diesel particulate emissions. SAE 760131.
- Wedel V. 1999. Technical Handbook for Marine Biodiesel in Recreational Boats, 2nd edition. Prepared for the National Renewable Energy Laboratory by Cyto Culture International, Inc., Point Richmond, CA.
- Wichmann HE, Peters A. 2000. Epidemiological evidence of the effects of ultrafine particle exposure. *Phil Trans Royal Soc London, Series A*, 2751-2768.
- Williams PT, Andrews GE, Bartle DG. 1987. The role of lubricating oil in diesel particulate and particulate PAH emissions. SAE 87084.
- Workshop of the International Life Sciences Institute (ILSI). 2000. The relevance of the rat lung response to the particles overload for human risk assessment: a workshop consensus report. *Inhal Toxicol* 12:1-17.